Intermediate-state structures of type-I superconductors

C. R. Reisin and S. G. Lipson
Department of Physics, Technion–Israel Institute of Technology, Haifa 32000, Israel
(Received 19 July 1999)

We have investigated pattern formation in the intermediate state of type-I superconductors, and have carried out accurate measurements of the dominant spatial periods of the patterns formed, including those related to a widely observed corrugated state. The relationship between the dominant spatial frequency and applied field is compared with the old theory of Landau from 1937 as well as to a recent theory proposed by Goldstein, Jackson, and Dorsey [Phys. Rev. Lett. **76**, 3818 (1996)] in which the Meissner state is replaced by current loops. The agreement with the latter model is significantly better than with earlier ones. We propose an alternative interpretation for the current-loop theory based on the representation of the field by Fourier series, which also gives us an understanding of the stability of small amplitude corrugations.

I. INTRODUCTION

Consider a bulk type-I superconductor of arbitrary geometry placed in a magnetic field $H<H_c$. Due to demagnetizing effects associated with the sample geometry, it can break into a number of normal and superconducting regions, forming very intricate patterns, known as the ''intermediate state.'' [1]

In a thin-plate sample normal to the applied field the static structure of the intermediate state usually shows two well-defined basic spatial periods that depend on the external applied field, and which presumably express the condition for the normal and superconducting phases to coexist side-by-side in equilibrium. There is a main period, the ''stripe'' period, describing a domain pattern, and a ''corrugation'' period (approximately half the strip period) describing an oscillatory structure within the stripe domains, which has not previously been adequately explained. In this work we present theoretical and experimental studies of the static equilibrium structures of this state. By using a representation of the magnetic field by Fourier series, we are able to explain quantitatively the stripe-period dependence on the applied field, as well as the conditions for which the corrugated state is stable.

In this work we present experimental studies of the period dependence of the intermediate-state structures in a bulk lead-indium alloy sample. The experiments were performed using magneto-optical techniques and image processing that allowed accurate measurements of the periodicity. The results were compared to an old model by Landau[2] and to a recent model by Goldstein, Jackson, and Dorsey,[3] which gives the same dependence as the Fourier representation. We found a significantly better agreement between the measured periodicity dependence and the latter theories than with the Landau theory. We also show that the corrugation period is roughly constant as a function of the applied field.

II. THEORY

A. Period dependence of the intermediate state

A theoretical treatment of the intermediate-state structure in superconductors was first given by Landau in 1937 (Ref. 2) prior to any experimental work. The Landau model, referred to as the ''nonbranching model,'' assumes that the intermediate state has a periodic laminar structure, in which the normal laminae near the surface broaden in order to reduce the magnetic energy above the surface, and that the field strength is H_c all over the interface boundary. Such structures arise from a competition between the magnetic-field energy, the condensation energy of the superconducting regions, and the interface energy between the normal and superconducting regions. Thus, the free-energy density in Landau's model is given by

$$F=F_0+\frac{H_c^2}{4\pi}\left[\frac{d\Delta}{a}+a f_L(h)\right], \tag{1}$$

with

$$f_L(h)=\frac{1}{4\pi}[(1+h)^4\ln(1+h)+(1-h)^4\ln(1-h) -(1+h^2)^2\ln(1+h^2)-4h^2\ln(8h)], \tag{2}$$

where $f_L(h)$ is the Landau function,[4] $h=H/H_c$ is the reduced field, a is the period of the structures, d is the thickness of the sample, and Δ is the surface energy parameter of the domain walls. The term F_0 represents the part of the energy that does not depend on a. The equilibrium period of the intermediate-state structures is obtained by minimizing the free energy (1) with respect to a

$$a=\left(\frac{d\Delta}{f_L(h)}\right)^{1/2}. \tag{3}$$

This model has been modified by assuming different shapes for the domains.[5–8] In 1957 Balashova and Sharvin[9] revealed that the normal domains, although basically laminar as pictured by Landau, were, in fact, corrugated in a way that no theory had taken into account. These more intricate patterns, documented in experiments, stimulated a re-examination of the theoretical problem. Faber[10] developed a ''corrugation model'' assuming that the lines of force cause a more intricate way of spreading out as they emerge from the sample than was assumed in Landau models, and that the

field energy should somehow include the surface energy parameter Δ, since it should control the amplitude of the corrugations. On comparing Faber's model and the ''nonbranching model,'' it can be seen that their predictions of the periodicity of the intermediate-state structures as a function of the reduced field do not differ much in shape. Since the interface energy Δ is not well known, it can be said that any set of experimental points which fits one theory can be scaled to fit the other.

Very little theoretical progress was made since Faber's model, and the extensive experimental data obtained so far has only qualitative agreement with the earlier theories.[11] Recently, Goldstein, Jackson, and Dorsey[3,12] (GJD) focused on the role of the demagnetizing fields in producing the observed patterns and developed a model in which the Meissner state is replaced by surface current loops (CL) and the field energy by Biot-Savart interaction between these loops. This model was developed in a general way, with no restriction to periodic patterns such as the laminar state, in analogy to models of other two-dimensional (2D) systems that exhibit patterns similar to the intermediate state. The ''CL model'' is based on domains bounded by current loops interacting as in free space and subjected to the constraint of constant total magnetic flux through the sample. As a result, GJD assumed that the magnetic part of the free energy of a sample has two contributions: that of the magnetization associated with current loops in the presence of the external field, and that of the self-induction and mutual induction of these loops.

GJD formulated the model for arbitrary domain shape and calculated the equilibrium periodicity for a laminar structure. When the laminae are assumed to have interfaces normal to the sample surface, they found a free energy similar in form to that in the ''nonbranching model'' (1), and therefore an equilibrium periodicity given by Eq. (3) but with $f_L(h)$ replaced by

$$f_{\mathrm{CL}}=\frac{1}{2\pi^3}\sum_{n=1}^{\infty}\frac{\sin^2(n\pi h)}{n^3}. \tag{4}$$

This function is slightly modified if the laminae are allowed to broaden as they approach the sample surface. The functions $f_L(h)$ and $f_{\mathrm{CL}}(h)$ have roughly similar forms and hence the equilibrium periods are close in the two models. One significant difference between the two functions is that the function $f_{\mathrm{CL}}(h)$ has an exact symmetry under the transformation $h\rightarrow 1-h$, a symmetry that is absent in the function $f_L(h)$. But it should be emphasized that although these two theories do give similar predictions for the periodicity as a function of the reduced field, they cannot be made to coincide by allowing an arbitrary choice of Δ.

We now present a different interpretation of the intermediate state based on the representation of the field by Fourier series; although this involves the same physics, and leads to the same results as the CL model, it gives an intuitive understanding of the origin of the corrugations. We assume the superconductor occupies the space $-d/2<z<d/2$. We represent the magnetic field in the region outside the superconductor by the reduced field $h(x,y,z)$, in units of H_c. The applied field is h, which has a value between 0 and 1. Initially we suppose that the intermediate state takes the form of

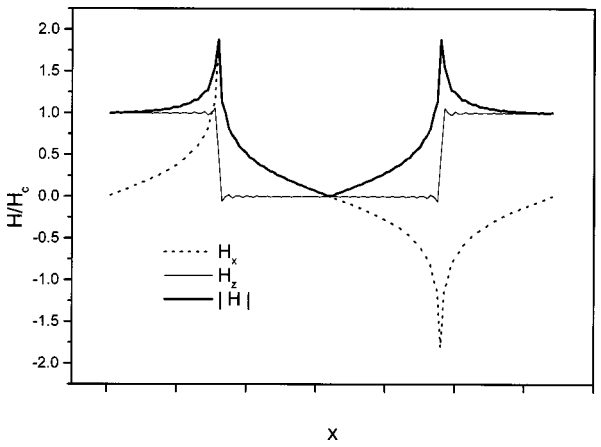

FIG. 1. Surface fields on a type-I superconductor in the intermediate state.

stripes parallel to y, with period a, such that the superconducting (Meissner) state occupies fraction $1-h$ and the normal part occupies fraction h. The interfaces are parallel to z. We require a magnetic field that satisfies the condition that $|h(x,y,z)|=1$ at all points on the surface of the normal regions and also $h_z=0$ at all points on the superconducting regions. Currents are induced in the superconductor causing a tangential field allowing the latter condition to be achieved (it is required for the Meissner effect) and these must have some effect on the surface field on the normal regions. Their effect there is quite small (Fig. 1) and results in an ''overshoot'' of the total field in the regions close to the n-s boundary, so that the former condition is not satisfied exactly. This can be rectified only by allowing a distortion of the interfaces. We shall therefore use an approximate representation of the field by a Fourier series, which is exact on the superconducting surface and therefore has this overshoot in the normal regions; however, at no point on the normal surface is $|h|<1$. This field has the form in the region $z>d/2$;

$$h_z(x,y,z)=\frac{1}{2}+\sum_{n=1}^{\infty}c_n\cos(2\pi nx/a)\times\exp[-2\pi n(z-d/2)/a], \tag{5}$$

which satisfies Laplace's equation. The values of c_n are determined by h. To satisfy Maxwell's equations, this must be accompanied by a second component;

$$h_x(x,y,z)=\sum_{n=1}^{\infty}c_n\sin(2\pi nx/a)\exp[-2\pi n(z-d/2)/a]. \tag{6}$$

These fields were used to construct Fig. 1 for the case $h=0.5$ in which case $c_n=(-1)^{(n-1)/2}/n\pi$ for odd n. The field energy arising from the nonuniformity of the field is then

$$\int_{d/2}^{\infty}|h|^2dz=\sum_{n=1}^{\infty}c_n^2a/4\pi n \tag{7}$$

per unit area, on one side of the sample, in units of $\mu_0H_c^2/2$.

For the continuation, we shall use Fourier transforms instead of series, the implication of a series being that the

transform consists of an array of δ functions of strength c_n. We can then make the following statements about the field at the surface of the specimen, in which A represents a unit area of integration,

$$\int \int_A h_z(x,y,d/2)dx\,dy = hA, \tag{8a}$$

$$\int \int_A h_z^2(x,y,d/2)dx\,dy = hA, \tag{8b}$$

since $h_z(x,y,z)$ has either unit or zero value at each point.

Let us represent the Fourier transform of $h_z(x,y,d/2)$ by $\tilde{h}(u,v)$ where (u,v) is the wave vector in the (x,y) plane and $w^2=u^2+v^2$. Then, since H_z satisfies Laplace's equation,

$$h_z(x,y,z) = \int \int \tilde{h}(u,v)\exp(-iux-ivy-wz)du\,dv. \tag{9}$$

Notice that since $\nabla \times H = 0$ the transforms of h_x and h_y are $iu\tilde{h}(u,v)/w$ and $iv\tilde{h}(u,v)/w$, respectively. In a two-dimensional model where $h_y=0$, the former transform becomes $i\,\mathrm{sign}(u)\tilde{h}(u,v)$.

The field excess per A (i.e., addition to that of the uniform applied field), taking into account also the energy due to h_{xy} which is equal to that of h_z, can be expressed in units of $\mu_0 H_c^2/2$ as

$$E_F = \int_{d/2}^{\infty} \int \int_A |h(x,y,z)|^2 dx\,dy\,dz$$

$$= \int \int |\tilde{h}(u,v)|^2/2w\,du\,dv. \tag{10}$$

We also note, from Parseval's theorem, that

$$\int \int |h_z(x,y)|^2 dx\,dy = \int \int |\tilde{h}(u,v)|^2 du\,dv, \tag{11}$$

and from Eq. (8b) this integral has the value hA.

Consider now the case of parallel-straight-striped domains with period $a=2\pi/u_0$. Then, $v=0$ and $w=|u|$. Fourier analysis with $u=nu_0$ gives

$$\tilde{h}(u) = \sum_{n>1} (n\pi)^{-1}\sin(n\pi h)\,\delta(u-nu_0). \tag{12}$$

Thus the field energy (10) is obtained with $w=nu_0$:

$$E_F = \sum_{n>0} \frac{\sin^2(n\pi h)}{(n\pi)^2}\frac{1}{2nu_0} \equiv \frac{\pi f_{\mathrm{FS}}(h)}{u_0}, \tag{13}$$

where

$$f_{\mathrm{FS}}(h) = \frac{1}{2\pi^3}\sum_{n=1}^{\infty}\frac{\sin^2(n\pi h)}{n^3}. \tag{14}$$

This recovers the result (4) of GJD for domains with walls normal to the sample surface, thus establishing the equivalence between the two models.

The interface energy per unit area due to the stripe pattern with the spatial frequency u_0 is

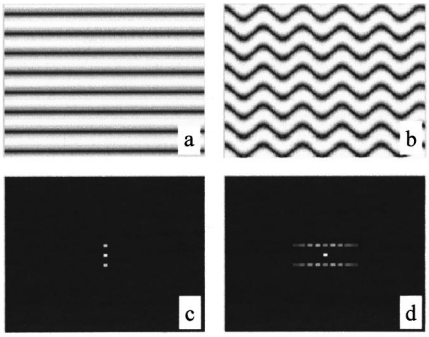

FIG. 2. Stripes and corrugations: (a) stripes; (b) corrugations; (c) Fourier spectrum of (a); (d) Fourier spectrum of (b).

$$E_S = \frac{d\Delta u_0}{\pi}. \tag{15}$$

The total energy E_F+E_S is minimized when the stripe period $a=2\pi/u_0$ is

$$a = \left(\frac{d\Delta}{f_{\mathrm{FS}}(h)}\right)^{1/2} \tag{16}$$

as obtained in (3).

B. Corrugation problem

We now consider a case in which the stripes are corrugated, by introducing nonzero values for v. Figures 2(a) and 2(b) show the straight and corrugated patterns schematically. Both are assumed to have the same value of h. The two-dimensional Fourier spectra of the two cases are also shown in Figs. 2(c) and 2(d). Because of the corrugations, each δ function on the u axis in Fig. 2(c) develops sidebands at multiples of the basic frequency v_0 of the corrugations in Fig. 2(d). We can easily compare the excess field energies in the two cases. The development of the sidebands increases the values of w for some of the terms of the field energy (10), and since the total value of $|\tilde{h}(u,v)|^2$ is preserved, Eq. (11), the total field energy is reduced by corrugation. It remains to show that the corresponding increase in interface energy does not always exceed this reduction.

The corrugated field, with amplitude ε at the interface, is best transformed in two stages:

$$h(x,y,z=d/2) = f(x-\varepsilon\cos v_0 y), \tag{17}$$

$$h(u,y,d/2) = \sum_{n>0}\frac{\sin(n\pi h)}{n\pi}\delta(u-nu_0) \times \exp[-iu\varepsilon\cos(v_0 y)], \tag{18}$$

$$h(u,v,d/2) = \sum_{n>0,m}\frac{\sin(n\pi h)}{n\pi}\delta(u-nu_0) \times J_m(\varepsilon n u_0)\,\delta(v-mv_0), \tag{19}$$

since the transform of $\exp[-iu\varepsilon\cos(v_0 y)]$ has orders m, with amplitude $(2\pi/v_0)J_m(u\varepsilon)$. For small enough ε, only $J_0(x) \approx 1-x^2/4$ and $J_1 \approx x/2$ need be included. Then the field energy for small $\varepsilon n u_0$ is

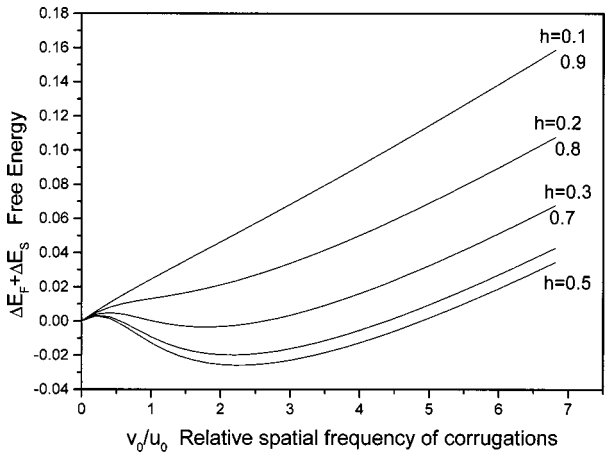

FIG. 3. Free energy $\Delta E_F+\Delta E_S$ [Eq. (24)] for $u_0 d=30$.

$$E_F \approx \sum_{n>0} \frac{\sin^2(n\pi h)}{(n\pi)^2} \times\left[\frac{[1-(\varepsilon n u_0)^2/4]^2}{2nu_0}+\frac{(\varepsilon n u_0)^2/2}{2\sqrt{n^2u_0^2+v_0^2}}+\cdots\right]. \quad (20)$$

It follows that the increase in field energy resulting from the corrugations (10) and (20) is, to order ε^2,

$$\Delta E_F \approx -\sum_{n>0} \frac{\sin^2(n\pi h)}{(n\pi)^2} \frac{(\varepsilon n u_0)^2}{2}\left[\frac{1}{2nu_0}-\frac{1}{2\sqrt{n^2u_0^2+v_0^2}}\right]. \quad (21)$$

It is clear that this series converges because at large n the terms approach those of Eq. (10).

The interface energy can be calculated directly, also to order ε^2. For the same geometry, with interfaces at $z=d/2$, $x=n\pi/u_0+\varepsilon\cos(v_0 y)$, the increase in length (per unit area of sample) is found by direct integration to be $\varepsilon^2 v_0^2 u_0/4\pi$. To minimize the interface area for given ε and v_0, the amplitude of the corrugations within the sample decays with z exponentially with decay length v_0^{-1}, so that the extra interface energy is

$$\Delta E_S=\frac{\Delta\varepsilon^2 v_0^2 u_0}{4\pi 2v_0}=\frac{\Delta\varepsilon^2 v_0 u_0}{8\pi}. \quad (22)$$

The total energy thus contains the uncorrugated terms (13) and (15), which are minimized by giving u_0 the value $2\pi/a$, and the corrugation terms (21) and (22), proportional to ε^2, with value,

$$\Delta E_F+\Delta E_S=-\sum_{n>0} \frac{\sin^2(n\pi h)}{\pi^2} \frac{(\varepsilon u_0)^2}{4}\left[\frac{1}{nu_0}-\frac{1}{\sqrt{n^2u_0^2+v_0^2}}\right] +\frac{\Delta\varepsilon^2 v_0 u_0}{8\pi}. \quad (23)$$

Substituting $\Delta=4\pi^2 u_0^{-2} f(h) d^{-1}$ from Eq. (16), we find that we must minimize,

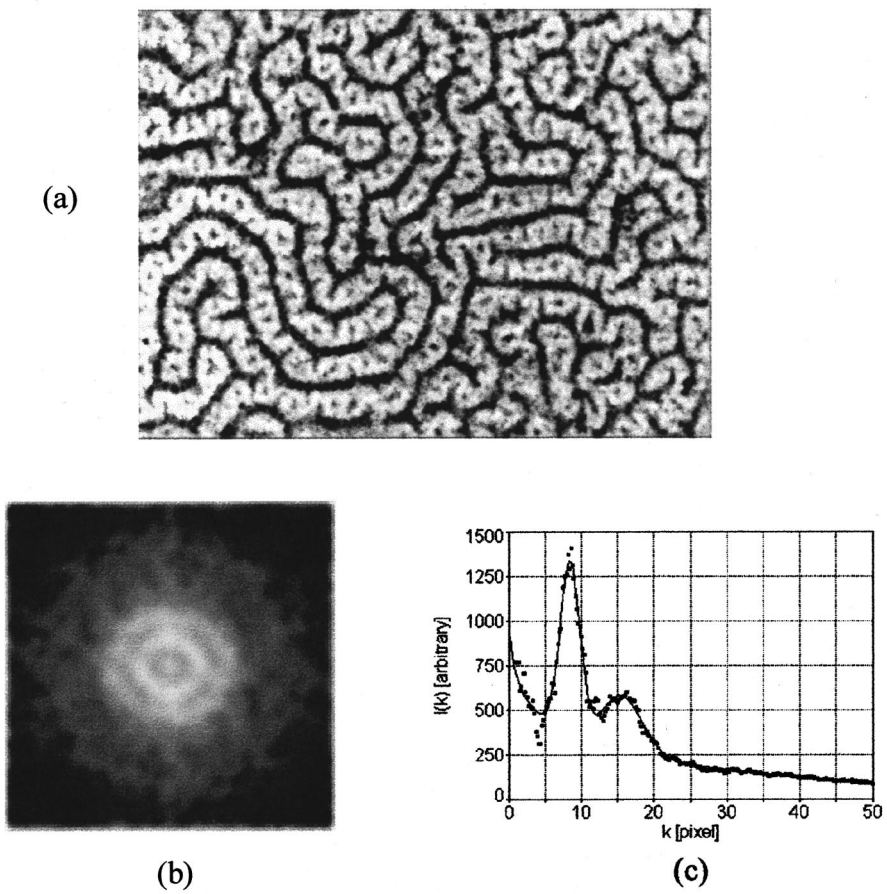

FIG. 4. Image analysis of corrugated pattern: (a) typical corrugated pattern, $h=0.53$. Normal regions are bright, superconducting regions are dark; (b) 2D FFT of (a); (c) spectral intensity–experimental points (●), fitted curve (——).

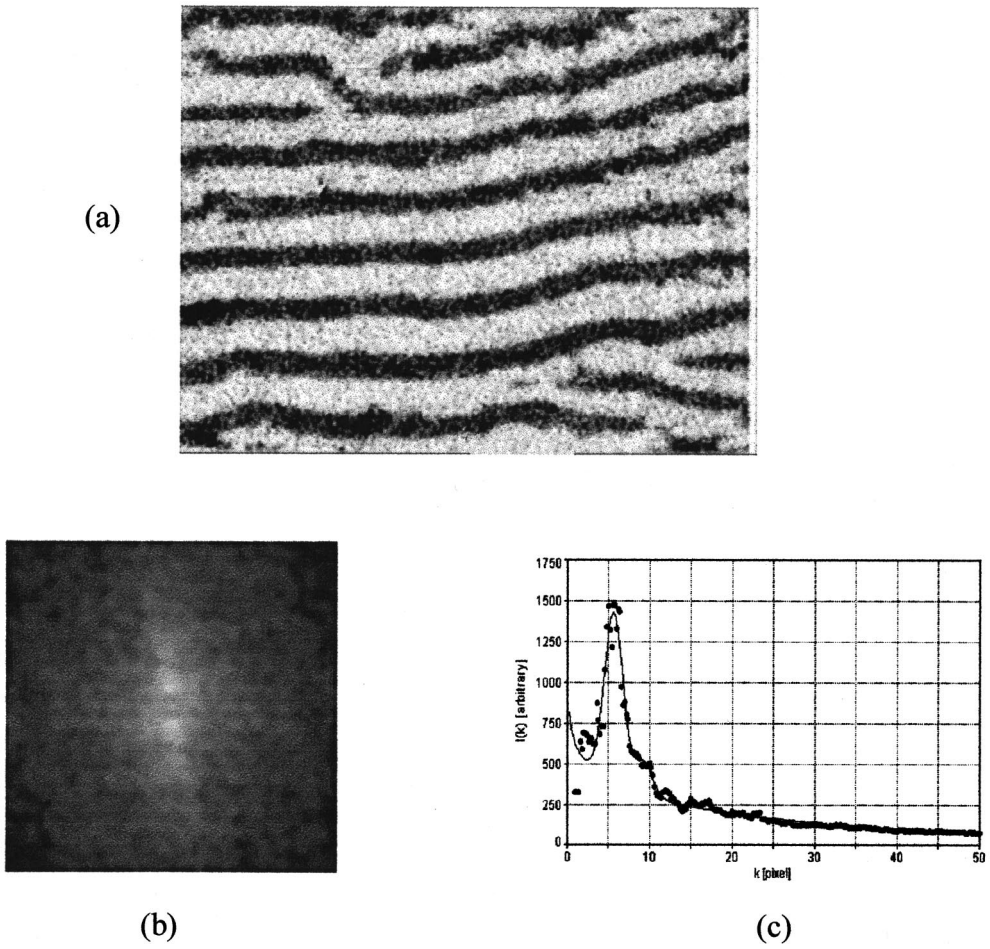

FIG. 5. Image analysis of laminar pattern: (a) typical corrugated pattern, $H=270$ G, $\beta=20°$. Normal regions are bright, superconducting regions are dark; (b) 2D FFT of (a); (c) spectral intensity–experimental points (●), fitted curve (——).

$$\Delta E_F+\Delta E_S=\frac{u_0\varepsilon^2}{4}\left\{\sum_{n>0}\frac{\sin^2(n\pi h)}{\pi^2}\left[\frac{1}{n}-\frac{1}{\sqrt{n^2+v_0^2/u_0^2}}\right]-\frac{2\pi v_0 f(h)}{u_0^2 d}\right\}. \tag{24}$$

It can be seen that this expression is a function of v_0/u_0 and $u_0 d$. Figure 3 shows an example of this function, for the case where $u_0 d=30$ at $h=0.5$, typical of the experiments. It can be seen that there is a distinct minimum, with a negative value of Eq. (24), at $v_0/u_0\cong 2$, which indicates the stability of small-amplitude corrugations under these conditions. In this approximation, the corrugations are stable only for $u_0 d>20$ at $h=0.5$, and the range of fields (symmetrically around $h=0.5$) for which they are stable increases with $u_0 d$. Moreover, it appears that the frequency v_0 of the minimum is approximately independent of the field as observed experimentally.

As already mentioned, the intermediate-state structure of a type-I superconductor in a perpendicular field [Fig. 4(a)] consists of domains with a well-defined periodicity but oriented isotropically. This results from the absence of any preferred orientation of a field component within the plane of the sample. A nearly ideal, straight laminar domain structure can be established experimentally by applying an inclined field [''Sharvin geometry'' (Ref. 13)]. Because of the field component parallel to the sample, the domain orientation is no longer isotropically distributed, but rather directed preferentially along the parallel field component. For this geometry the periodicity expressions (3) and (16) are modified to[13]

$$a=\left(\frac{d\Delta}{f_L(C_N)}\right)^{1/2}(C_N^2\cot^2\beta+1)^{1/2}, \tag{25}$$

where

$$C_N=\frac{H_x}{(H_c^2-H_z^2)^{1/2}}=\frac{h\sin\beta}{(1-h^2\cos^2\beta)^{1/2}}$$

is the bulk fraction of the sample in the normal state and β is the angle between the applied field and sample surface.

III. EXPERIMENTAL SYSTEM

We now present experimental studies of the static equilibrium state of the intermediate-state structures of a bulk lead-indium alloy sample, for both corrugated and laminar patterns. In the following, we describe the experimental system used for the direct observation of flux penetration into type-I superconductors.

The experimental setup developed for the current research is divided into three basic parts—an optical system, a cry-

ostat, and a magnetic-field generator. The studies were carried out in a miniature continuous-flow helium cryostat placed on a polarizing microscope. The intermediate-state structures were observed by means of the magnetooptical Faraday effect using EuSe evaporated on an optical window as the magneto-optical active material.[14] The investigated sample was a disk of bulk Pb+0.5-wt% In, 3 mm diameter and 0.14 mm thickness. The sample was prepared by melting together high purity materials, and was annealed and chemically polished. Susceptibility measurements were performed on the sample in order to determine its critical temperature, which was found to be $T_c = 7.18\,\mathrm{K}$. The external field was generated by a set of magnetic coils, so that the perpendicular and the parallel components of the field were controlled independently. The patterns were photographed by a video camera, recorded on a video tape, and then analyzed by computer.

IV. DATA ANALYSIS

We achieved a sufficiently high accuracy of measurement to distinguish between the predictions of equilibrium periodicities of the Landau and CL theories by use of a high-contrast magneto-optical observation technique and spatial frequency analysis of the images. The magneto-optical technique offers the possibility of observing static and dynamic processes with 1-μm resolution. Digital-contrast-enhancement methods were used to increase the visibility of the detailed information, and spatial frequency analysis of complete images, based on a two-dimensional fast-Fourier-transform (FFT) method, was used for the determination of the equilibrium periodicities.

The Fourier transform of a real image is a centrosymmetric function $F(u,v)$ with peaks at the characteristic frequencies of the pattern and at the origin (zero-order peak). The spectral intensity is

$$I(k) = \int_0^\infty \frac{|F(u,v)|^2 \delta[(u^2+v^2)-k^2]}{2\pi k}\, du\, dv. \qquad (26)$$

The characteristic frequencies are extracted by fitting $I(k)$ to two Gaussian peaks, and a smooth background. The reason for fitting $I(k)$ to two Gaussian functions is that the corrugated patterns show two distinct wavelengths, that of the ''stripes'' and that of the corrugations of the individual domains. The image analysis allowed us to measure both periodicities simultaneously. A typical example of the image analysis of a corrugated pattern is presented in Fig. 4. The 2D FFT of the pattern shows two annular peaks at two different frequencies $|k_1|$ and $|k_2|$ corresponding to the periodicity of the structures and the corrugation wavelength, respectively. The annular forms of the peaks are due to the absence of any preferred domain orientation in these patterns. The spectral intensity function was found by applying Eq. (26), after which the frequencies were extracted and the periodicities were calculated. After applying the image analysis method to laminar patterns, the 2D FFT of the pattern had two peaks around $\pm k$, corresponding to a single characteristic periodicity of these patterns (Fig. 5). The periodicities could be measured to an accuracy of about 1%.

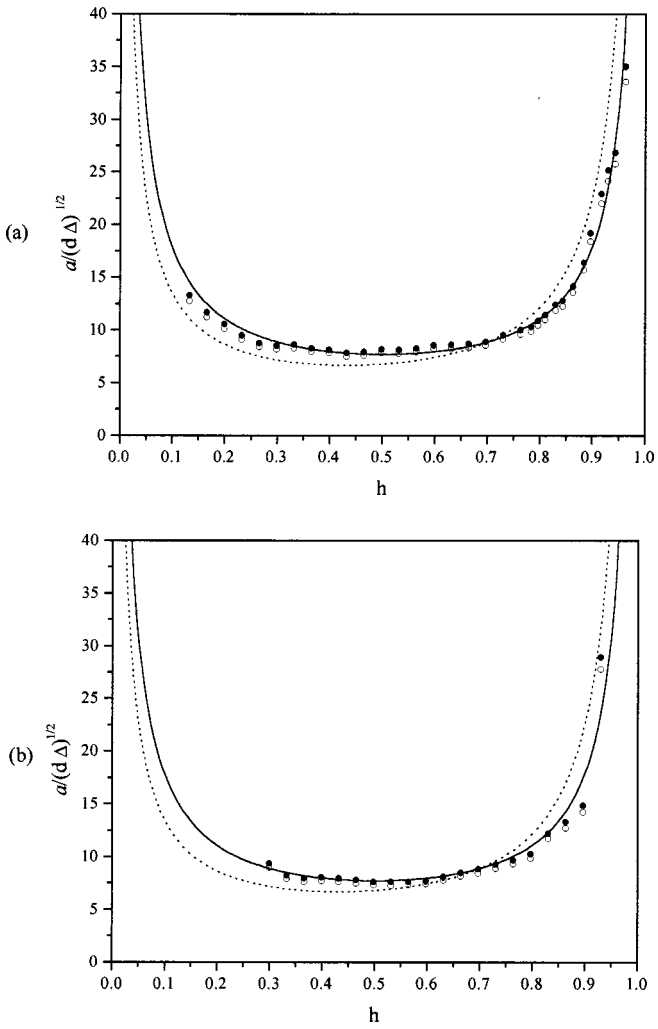

FIG. 6. Periodicity of corrugated structures as a function of the reduced field, Landau model (− − −), and CL model (——). The points are the experimentally observed periodicities scaled using Δ_L (○) and Δ_{CL} (●): (a) $(NI)_T$ transition; (b) $(SI)_T$ transition.

V. PERIOD DEPENDENCE OF THE INTERMEDIATE STATE STRUCTURES

The equilibrium patterns of the intermediate-state structures were recorded as a function of the applied field and analyzed as described above. The results were compared to Landau's model, Eq. (2) and Eq. (3), and to the CL model, Eq. (14) and Eq. (16), which predict a close but different form of the period dependence in the equilibrium state.

Corrugated pattern: The domain patterns show two distinct wavelengths, that of the ''stripes'' and that of the corrugations of the individual domains. The image analysis allowed us to measure both periodicities simultaneously.

The experiment was performed at a temperature $T = 4.62\,\mathrm{K}$ with the sample within a homogeneous magnetic field applied perpendicular to the sample surface. The intermediate state was established at a constant temperature by raising the field from zero [$(SI)_T$ transition] and by lowering the field from above H_c [$(NI)_T$ transition]. The domains consist of domains of well-defined periodicity but oriented isotropically. The periodicities of the structures of the $(NI)_T$ and $(SI)_T$ transitions were measured as a function of the applied reduced magnetic-field strength $h = H/H_c$. Since it

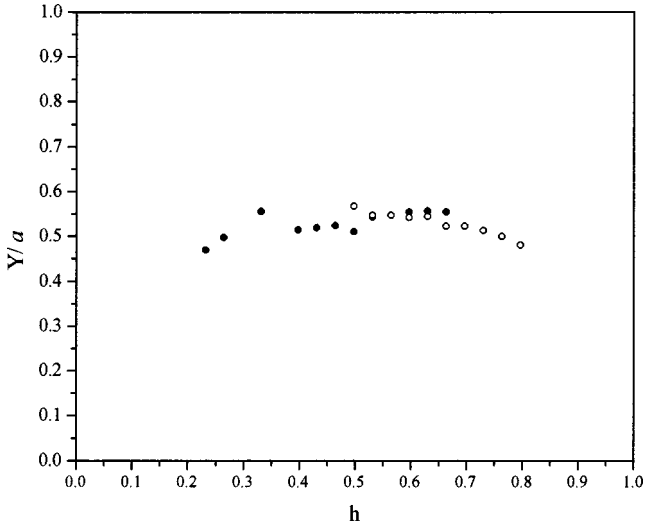

FIG. 7. Ratio between corrugation wavelength and structure periodicity as a function of the reduced field for $(NI)_T$ transition (●) and $(SI)_T$ transition (○).

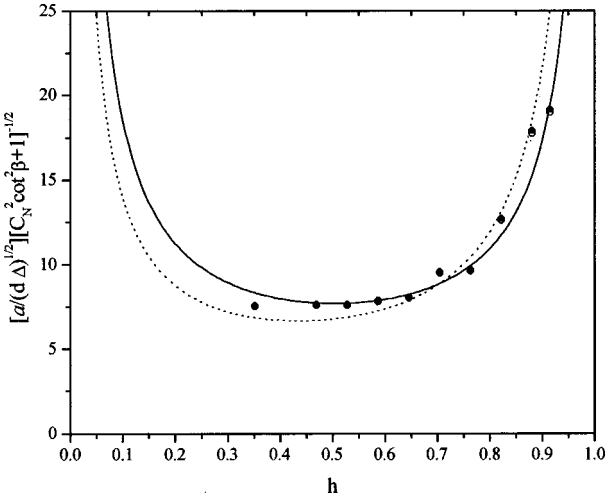

FIG. 8. Periodicity of laminar structures as a function of the reduced field, Landau model (− − −) and CL model (——) for Sharvin's geometry. The points are the experimentally observed periodicities scaled using Δ_L (○) and Δ_{CL} (●) [$(NI)_T$ transition].

was not possible to measure the critical field H_c at the temperature of the experiment with any precision, it was obtained by extrapolation of the reciprocal value of the periodicity as a function of the applied field. We obtained $H_c(T=4.62\,\mathrm{K})=335\pm5$ G.

Figure 6 shows the experimental results of the periodicity of the structures as a function of the reduced field *h*, for $(NI)_T$ and $(SI)_T$ transitions compared with the curves predicted by Landau and by the CL model. The experimentally observed periodicities were scaled to the different models by calculating the best values for the surface energy parameter. The value $\Delta_L=839\pm33$ Å was obtained for the Landau model and $\Delta_{\mathrm{CL}}=771\pm32$ Å for the CL model at $T=4.62$ K. The experimental results show significantly better agreement with the period dependence of the intermediate-state structures according to the CL model. A significant difference between the period of the structures of the $(NI)_T$ and $(SI)_T$ transitions was not found.

One interesting point to note is that at low fields at the $(SI)_T$ transition, the patterns consist of macroflux droplets of different diameters. This phenomenon was observed by Goren and Tinkham[15] who showed that the energy difference between such a state and a periodic state is very small. It may be nucleated at low fields by small local variations in the physical properties (such as thickness or composition) of the film or in the path followed when entering the state.

Figure 7 shows the ratio between the corrugation wavelength and the structure periodicity as a function of the reduced field. It can be seen that within the experimental error, it is constant with a mean value of 0.52 ± 0.02, which can be compared with the model value of approximately 0.5 in the region of fields shown (Fig. 3).

Laminar domain structures were established by applying an inclined field. Because of the field component parallel to the sample, the domain orientation is directed preferentially along the parallel field component. The technique adopted in this experiment was to keep the parallel component of the field constant at 269 ± 5 G while the perpendicular component was varied independently. The experiment was performed at $T=4.67$ K.

The period of the laminar structures was measured as a function of the applied reduced field in $(NI)_T$ transition. The critical field $H_c(T)$ was obtained by using the empirical temperature dependence $H(T)=H_o[1-(T/T_c)^2]$.

Figure 8 shows the experimental results scaled using $\Delta_{\mathrm{CL}}=755\pm65$ Å and $\Delta_L=758\pm65$ Å obtained by fitting the data to the CL and Landau's models, respectively. The results were compared with the Landau model and the CL model using Sharvin's extension for inclined-field geometry (25). Once again we found a significantly better experimental agreement of the period dependence of the intermediate-state structures with the CL model, and that the data cannot be scaled to fit the Landau model within the experimental error by a single value of Δ.

Finally, we can compare the values of the surface energy parameter obtained in the corrugated and laminar patterns by calculating the surface parameter energy at $T=0$ K using the temperature-dependence function $\Delta(T)=\Delta_0(1-T/T_c)^{-1/2}$. The values agreed well: $\Delta(T=0)=460\pm20$ Å and $\Delta(T=0)=446\pm38$ Å, respectively.

VI. CONCLUSIONS

We investigated the pattern formation of the intermediate state in type-I superconductors on both corrugated and laminar domain structures. This paper deals with the static aspect of the phenomena.

We developed an image-processing analysis method for accurate determination of the period dependence of the intermediate-state structures from magneto-optic images. Using this method on both corrugated and laminar domain structures, we have shown that the measured periodicities are in significantly better agreement with Goldstein *et al.*'s current loop model than with Landau's nonbranching model. In addition, we have proposed a simple extension of the CL model to explain the observation of a corrugated state when the field is normal to the sample.

ACKNOWLEDGMENTS

We are grateful to R. E. Goldstein and A. T. Dorsey for useful discussions. We thank S. Hoida for technical assistance. We also wish to thank A. Forkl and T. Dragon for their assistance, A. Knizhnik for his help preparing the sample, and Y. Direktovich for measuring the critical temperature of the sample. The research was carried out with the support of German-Israel Research Foundation, the Minerva Foundation for Nonlinear Science, and the Crown Center for Superconductivity.

[1] R. P. Huebener, *Magnetic Flux Structures in Superconductors* (Springer-Verlag, New York, 1979).
[2] L. D. Landau, Zh. Eksp. Teor. Fiz. **34**, 537 (1958) [Sov. Phys. JETP **7**, 371 (1937)].
[3] R. E. Goldstein, D. P. Jackson, and A. T. Dorsey, Phys. Rev. Lett. **76**, 3818 (1996).
[4] A. Fortini and E. Paumier, Phys. Rev. B **5**, 1850 (1972).
[5] L. D. Landau, J. Phys. (USSR) **7**, 99 (1943).
[6] E. R. Andrew, Proc. R. Soc. London, Ser. A **194**, 98 (1948).
[7] C. G. Kuper, Philos. Mag. **42**, 961 (1951).
[8] E. M. Lifshitz and Iu. V. Sharvin, Dokl. Akad. Nauk **79**, 783 (1951).
[9] B. M. Balashova and Iu. V. Sharvin, Zh. Eksp. Teor. Fiz. **31**, 40 (1959) [Sov. Phys. JETP **4**, 54 (1957)].
[10] T. E. Faber, Proc. R. Soc. London, Ser. A **248**, 460 (1958).
[11] A. Kiendl and H. Kirchner, J. Low Temp. Phys. **14**, 349 (1974); D. E. Farrell, R. P. Huebener, and R. T. Kampwirth, *ibid.* **19**, 99 (1975); A. Kiendl, *ibid.* **38**, 277 (1980).
[12] A. T. Dorsey and R. E. Goldstein, Phys. Rev. B **57**, 3058 (1998).
[13] Iu. V. Sharvin, Zh. Eksp. Teor. Fiz. **33**, 1341 (1958) [Sov. Phys. JETP **6**, 1031 (1958)].
[14] B. Dutoit and L. Rinderer, Jpn. J. Appl. Phys., Part 1 **26**, 1661 (1987); Th. Schuster, M. R. Koblischka, B. Ludescher, N. Moser, and H. Kronmuller, Cryogenics **31**, 811 (1991); M. R. Koblischka and R. J. Wijngaarden, Supercond. Sci. Technol. **8**, 199 (1995).
[15] R. N. Goren and M. Tinkham, J. Low Temp. Phys. **5**, 465 (1971).